Biosensors and Bioelectronics 91 (2017) 721–727

Contents lists available at ScienceDirect

Biosensors and Bioelectronics

journal homepage: www.elsevier.com/locate/bios

On-chip electrochemical immunoassay platform for specific protein biomarker estimation in undiluted serum using off-surface membrane matrix

Sunil K. Arya*, Patthara Kongsuphol, Mi Kyoung Park

*Institute of Microelectronics, Agency for Science Technology and Research (A*STAR), 2 Fusionopolis Way, #08-02 Innovis Tower, Singapore 138634, Singapore*

ARTICLE INFO

Keywords:
Electrochemical sensor
Off-surface 2D matrix
Poly carbonate, FNAB
TNF-α
Serum

ABSTRACT

The manuscript presents a new biosensor platform using bioreceptors modified porous 2-dimensional (2D) membrane based off-surface matrix for on-chip electrochemical immunoassay. Antibody based bioreceptors modified 2D matrix of porous polycarbonate (PC) membrane with densely packed 20 μm holes as off-surface matrix was incorporated in very close proximity of the sensor surface and integrated with fluidic system for reagent flow and incubation chamber. Covalent attachment of antibodies on 2D PC membrane based off-matrix was achieved using 4-fluoro-3-nitro-azidobenzene (FNAB) cross-linker. Anti-TNF-α/FNAB/PC membrane was integrated over array of micro fingers of gold based sensor chip using double side tape spacer and StartingBlock phosphate buffer saline- Tween-20; (PBS-T20) blocking buffer was utilized to minimize nonspecific binding. Differential pulse voltammetric studies of Anti-Tnf-α/FNAB/PC-Au for protein biomarker (TNF-α) detection and estimation in undiluted serum indicated that the immunosensor system can detect TNF-α linearly in 100 pg/ml to 100 ng/ml range with insignificant interference from other cytokines and serum proteins. Further, immunosensor exhibited high sensitivity of 194 nA/(ng/ml) and 240 nA/(ng/ml), respectively for single and double membrane based system. Thus, use of 2D membrane based off surface matrix may present the new platform to sensitively measure biomarkers electrochemically to pg/ml range with insignificant nonspecific binding and false signal in undiluted serum.

1. Introduction

Proteins, the building blocks of all living organisms, in appropriate range are crucial for healthy life, however their lower or higher level disturbed biological state and health of living being. This lower and higher level of proteins associated with various disorders has provided the opportunity to researcher to use them as biomarkers for prognosis and diagnosis of disease and to monitor effect of medicines during treatment (Arya and Bhansali, 2011; Chikkaveeraiah et al., 2012; Felder et al., 2014; Guo et al., 2015). Various proteins have already been established as biomarkers and have shown the promise of early and accurate prognosis of disease via their rapid and quantitative estimation using various methods (Chikkaveeraiah et al., 2012; Li et al., 2010). Further, the level of protein markers is known to increase with the stage of disease and its measured level can be correlated to disease stage accurately in most cases.

In recent years, immunosensors has shown great promise to be used as effective methods for protein detection and can potentially result in point-of-care (POC) device developments (Corrie et al., 2015; Kaushik et al., 2014; Vasan et al., 2013). Immunosensors can be tailored with newly researched and developed protocols for recognition molecule binding and desired target detection methods to realize improved, reliable and rapid disease diagnosis (Arya et al., 2013, 2012; Bosnjakovic et al., 2012; Liu et al., 2015a; Mazloum-Ardakani and Hosseinzadeh, 2015; Sun et al., 2013). Among various immunoassay detection methods, electrochemical ELISA based detection, which utilizes specificity of optical ELISA and simple fabrication, higher sensitivity, low cost and direct transduction of signal for electrochemical system has gained interest in development of electrochemical immunosensors (Fei et al., 2015; Gan et al., 2011b; Li et al., 2015; Mazloum-Ardakani et al., 2015; Pan et al., 2017; Sadik et al., 2009; Wei et al., 2016). However, fabrication of such biosensors usually involve binding of bio-recognition molecule on the surface of sensing electrode (Kokkinos et al., 2016; Pan et al., 2017; Zhang et al., 2016), which may cause fouling of sensor surface, and degradation of bio-recognition molecule during measurement scan in case of electroche-

* Corresponding author.
E-mail address: sunilarya333@gmail.com (S.K. Arya).

http://dx.doi.org/10.1016/j.bios.2017.01.033
Received 7 December 2016; Accepted 17 January 2017
Available online 18 January 2017
0956-5663/

mical sensing. Also, it has been observed that surface modification or immobilizing non-conducting bioreceptors such as antibodies or enzyme for selectively capturing target molecules decrease the conductivity of sensing electrode or sometime make them insulating, thus may reduce its ability to detect electrochemical signal sensitively (Arya et al., 2014; Arya and Park, 2014). Furthermore, measurement in real samples like serum, which have large number of highly concentrated non-target proteins may cause large background and false signal. Thus, there is an opportunity to design a electrochemical ELISA based system for enhanced signal detection (Li et al., 2015; Pan et al., 2017; Salimi et al., 2014; Zhang et al., 2016), while avoiding other issues and to measure signal sensitively and selectively especially in real samples.

To avoid the issues related to serum proteins, researchers have used the diluted serum (Gan et al., 2011a), however such step also dilute the desired protein concentration thus, make it difficult to be detected. On other hand to avoid the issues due to surface modification in electrochemical sensors, researchers have tried modifying the surface between or adjacent to electrode (Wang et al., 2014), however, such approach also result in exposure of active sensor surface to various modification reagents, which can adsorb on sensor to give false or varying results. Thus, efforts are required to develop new system, which can avoid these issues, while improving the sensor characteristics.

To develop electrochemical immunosensor without above mentioned issues, this paper describe the use of our recent patent on off-surface matrix based on-chip measurement (Arya et al., 2016), for detection of TNF-α in undiluted serum. There are various approaches have been developed for TNF-α detection (Li et al., 2012; Liu et al., 2015b; Pei et al., 2011; Wang et al., 2006; Yin et al., 2011), however in present work, it is taken as model marker to demonstrate off-surface matrix concept. The approach involves the selection and modification of matrix before attaching on sensor surface using spacer. In present work, 2-dimensional (2D) porous membrane of polycarbonate (PC) with densely distributed 20 μm holes has been chosen for its off-site modification with antibody followed by on-chip electrochemical detection of TNF-α (protein marker) in undiluted serum. Off-surface 2D matrix was first modified with bioreceptor using cross linker (4-fluoro 3-nitro azidobenzene (FNAB)) at remote location and then arranged and packaged in near vicinity of sensor surface via few micron thick spacer for fluidic flow and electrochemical sensing in undiluted serum samples with high specificity, and negligible interference from other proteins. Fig. 1 shows the images of PC membrane at various steps of modification with cross-linker and schematic for matrix modification with anti-TNF-α antibody. Results of present study reveal the potential of such approach to replace gold standard of optical ELISA at present.

2. Materials and methods

2.1. Chemicals

4-Aminophenyl phosphate monosodium salt (4-APP) was procured from Santa Cruz Biotechnology (USA). Antibodies and proteins were procured from Biolegend (USA); StartingBlock phosphate buffer saline-Tween 20; (PBST20) and StartingBlock tris base saline-Tween 20; (TBST20) were from fisher scientific, streptavidin-conjugated alkaline phosphate (ALP) solution was from Mabtech AB; Femto TBS procured from G-Biosciences. FNAB was from Setareh Biotech, LLC, polycarbonate membrane filter containing 20 μm holes was procured from sterlitech. Other analytical grade chemicals were utilized as received.

2.2. Gold electrode construction

Gold electrodes patterned in comb shape were created using microfabrication techniques and lithographic on thermally grown oxide layer coated silicon wafers (Pui et al., 2013). 5 μm wide and 3200 μm long comb fingers separated by 25 μm space were patterned over 5500 μm long base and utilized as sensors. The fabricated comb shaped gold electrodes were washed with ethyl alcohol, acetone and sufficient amount of water and then treated with UV-ozone for 30 min before use.

2.3. PC membrane and its modification using cross-linker

Off-surface matrix made of PC membrane was prepared via laser cutting of large filter into smaller matrix of oval shape with longer width of 9 mm and smaller width of 7 mm. Laser cut membrane was first cleaned with water and methanol followed by drying in air (Fig. 1a). Cleaned PC matrix was then modified with FNAB via photochemical reaction. 1 mg of FNAB in 25 μl of methanol was found to be optimal quantity for each PC membrane surface modification as higher concentration resulted in same response. FNAB solution in methanol was dropped on PC matrix and allowed to dry in dark (Fig. 1b). After drying, membranes were UV treated for 10 min using UV curing setup from Dyna tech (DT-UIS 1020) (Fig. 1c) and then washed with methanol to remove extra FNAB (Fig. 1d). FNAB has been used as cross linker to covalently immobilize antibodies and nitrene reaction occurring at azido group of FNAB during UV irradiation results in insertion of FNAB into C–H bond of PC matrix (Bora et al., 2006). Change in color of PC membrane at every step of FNAB treatment confirmed its modification (Fig. 1a-d).

2.4. Immobilization of anti-TNF-α antibody on FNAB modified PC membrane

Stock solution of 10 μg/ml anti-TNF-α antibody was prepared in phosphate buffer saline solution (PBS) (1x). For covalent immobilization, various volume of antibody solutions were tested and 25 μl was found to be optimum as it is found to cover whole membrane and no drying effect was observed during incubation at 37 °C in humid chamber for 2 h binding process. Thus, for antibody binding each membrane was submerged in 25 μl of Anti-TNF-α antibody stock in PBS and incubated at 37 °C for 2 h in humid chamber. During the incubation thermal replacement of active fluoro group occur by nucleophilic attacking amino group of antibody resulting in covalent immobilization of antibody on PC membrane via FNAB cross-linker (Arya et al., 2006, 2007; Bora et al., 2006). After antibody immobilization, membranes were washed with PBS-tween 20 solution and with PBS to remove non-cross-linked antibodies. Anti-TNF-α/FNAB/PC membrane was then integrated on sensor surface followed by blocking free spaces and preventing non-specific binding via 30 min incubation of starting block PBS T20 (SB) blocker. Fig. 1e shows the schematic for matrix modification and antibody binding.

2.5. Assembly of modified PC membrane on chips and development of off surface matrix with on-chip measurement system

Modified PC membranes were assembled on Au electrode chip using cleaned laser cut double sided tapes. For assembly, 9 mm×11 mm size double sided tape was laser cut to create oval shape chamber with longer width of 8 mm and smaller width of 6 mm. Oval shape was selected for better fluidic flow and to avoid dead fluid. Each modified membrane was sandwiched between two double sided tapes in which one or two membranes were used to create the off surface matrix with on-chip measurement system (Fig. 2a). Finally, to make fluidic and incubation chamber, 9 mm x 11 mm size PMMA sheet with two holes was placed on top of membrane using double sided tape. The Anti-TNF-α/FNAB/ PC-Au electrode thus formed were stored at 4 °C in humid chamber when not in use. Fig. 2 shows the schematic for integrated modified PC membrane on sensor chip along with schematic steps for immunoassay.

2.6. Immunoassay process sequence

Schematic in Fig. 2b shows the various steps involved in immu-

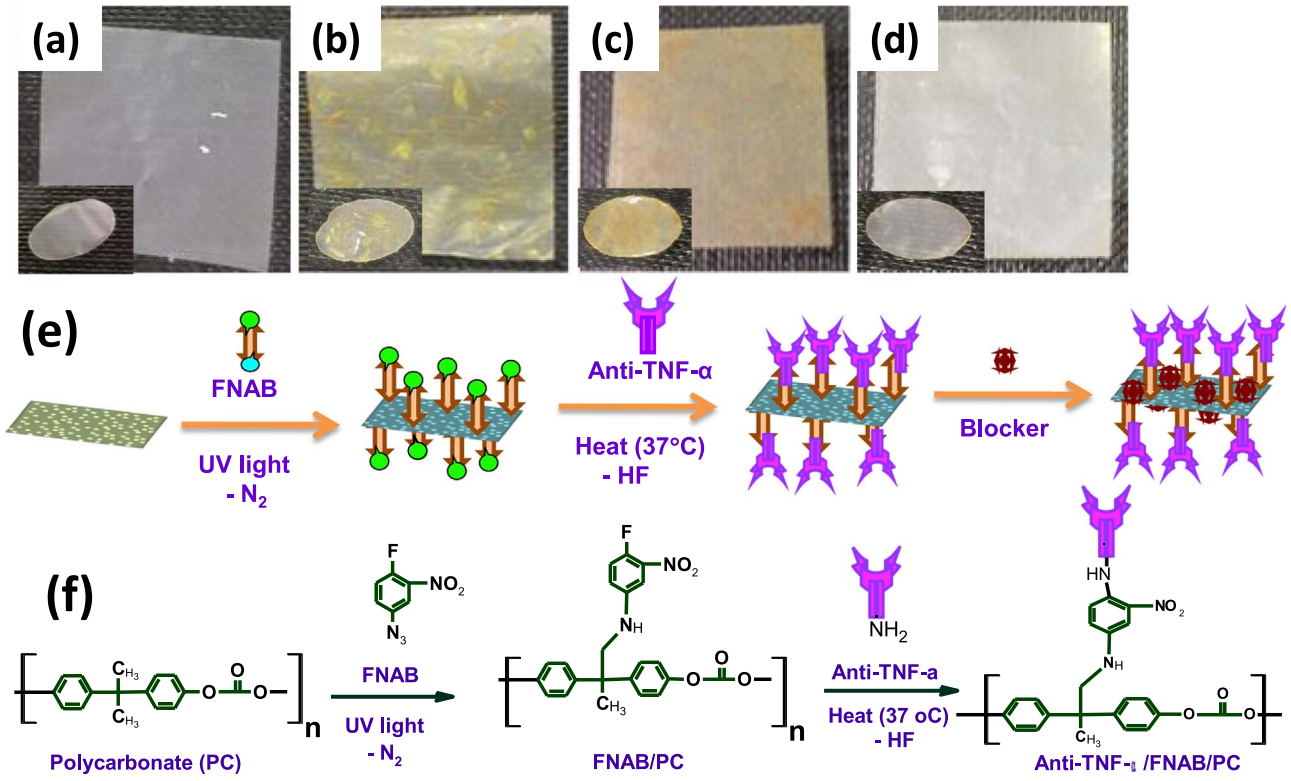

Fig. 1. PC membrane at various stages of FNAB modification (a) blank, (b) after dropping FNAB and drying in dark, (c) after UV exposure and (d) after washing with methanol, (e) schematic for PC based off-surface matrix modification with capturing biomolecule, and (f) chemical reaction schematic for surface modification. (For interpretation of the references to color in this figure, the reader is referred to the web version of this article.)

noassay, briefly 20 µl of undiluted serum with desired TNF-α concentration was incubated in the incubation chamber, where TNF-α interacted with Anti-TNF-α modified FNAB/PC-Au electrode. After optimized 20 min of incubation, chip was washed three times using 0.5 ml/wash of 1x Femto TBST washing buffer and extra solution was removed. After antigen-antibody interaction, chip was incubated with 20 µl of 10 µg/ml biotin conjugated secondary anti-TNF-α antibody solution in starting block TBST20 for another 20 min, where secondary anti-TNF-α binds to antigen at different epitope from captured antibody. On completion of incubation period chip was again washed in same way as after first incubation and then allowed to interact with 20 µl of 10 µg/ml streptavidin-alkaline phosphatase solution in starting block TBST20 for next 20 min, where streptavidin-alkaline phosphatase bind to secondary anti-TNF-α antibody via biotin-streptavidin

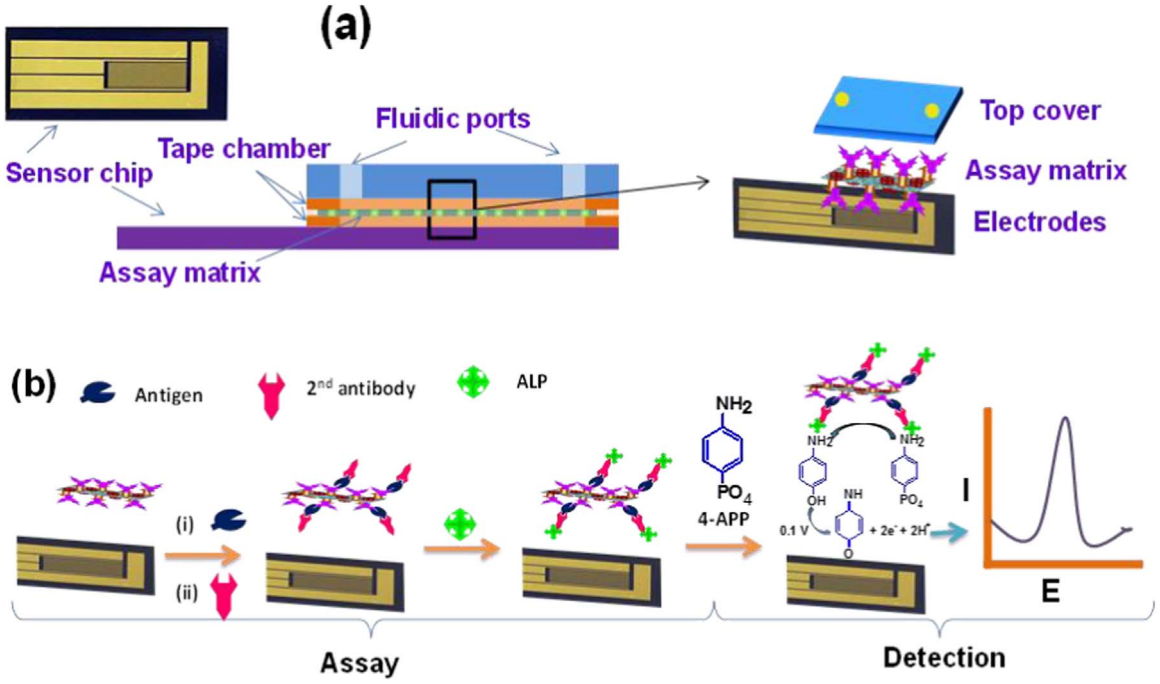

Fig. 2. (a) Schematic for modified PC membrane integrated on sensor chip, (b) schematic steps for immunoassay.

specific interaction. Streptavidin-alkaline phosphatase binding was followed by washing and final 20 min incubation with 2 mg/ml 4-APP in deoxygenated tris-HCl buffer (100 mM, pH 9) containing 4 mg/ml $MgCl_2{\cdot}6H_2O$. After 4-APP incubation, voltammetric (differential pulse voltammetric; DPV) signal was recorded using DPV in voltage scan in −0.3–0.4 V range, with 25 mV of amplitude, 10 mV of step potential, and 0.1 s of interval time. Autolab Potentiostat/Galvanostat from EcoChemie, Netherlands running on General Purpose Electrochemical System (GPES) software v4.9 was used to perform DPV scan. Undiluted serum as control and serum spiked with other cytokines such as IL6, IL8 and IFN-γ were used for interference studies. All studies were repeated at least three times and data's were represented as error bars.

3. Results and discussions

3.1. Anti-TNF-α/FNAB/PC-Au electrode and its working principle

Fig. 1 shows the schematic for 2D laser cut PC membrane and its modification, where FNAB provides link between anti-TNF-α antibody and PC membrane. Binding of antibody to FNAB modified PC membrane resulted in change in the membrane property. Hydrophobic character of FNAB modified PC membrane became hydrophilic following antibody binding. Change in color of PC membrane after FNAB binding and change in hydrophobic to hydrophilic character after anti-TNF-α binding indicated successful modification at each step. To develop off-surface matrix for on-chip measurement, antibody modified membrane was integrated on sensor. Fig. 2 shows the schematic for integrated sensor with modified PC matrix sandwich between sensor surface and top PMMA cover. Double sided tape provided spacer between modified membrane and the sensor chip and it formed an incubation chamber between modified membrane and top PMMA sheet. The steps of immunoassay have been schematically represented in Fig. 2b, where reagents bind in sequential manner to finally produce ALP catalyzed product of 4-APP, which upon applying potential via DPV produces current. Separation of antibody-antigen binding matrix from sensor surface resulted in improved sensitivity with low background response.

3.2. Blank gold sensor chip characterization

Blank gold sensor chip was characterized using cyclic voltammetry (CV) in PBS (1x) containing 5 mM potassium ferrocynide- 5 mM potassium ferricynide ($FeCN_6^{3-/4-}$). Fig. 3a showing CV scan of blank sensor chip reveal semi reversible behavior with similar oxidation and reduction peak currents. Inset of Fig. 3a showing Nyquist plot of impedance scan in PBS containing 5 mM $FeCN_6^{3-/4-}$ reveals low charge transfer resistance (190 Ω) for clean blank chip. Chip was further investigated under different scan rates (30–100 mV/s) (Fig. 3b) and linear increase in oxidation and reduction peak currents with square root of scan rate (inset (i) in Fig. 3b) obeying Eqs. (1) and (2) suggested diffusion controlled process on sensor surface. Further, the linear variation in potential difference between oxidation and reduction peaks (inset (ii) in Fig. 3b) suggested the easy electron movement from medium to mediator (Vasudev et al., 2013).

$$I_{oxi}\ (\mu A) = -\ 9.64\ \mu A + 23.20\ (Scan\ rate)^{1/2}\mu A;\ \ R = 0.998 \ldots\ldots \quad (1)$$

$$I_{red}\ (\mu A) = -\ 1.04\ \mu A + 22.3423.20\ (Scan\ rate)^{1/2}\mu A;\ \ R = 0.998 \ldots\ldots \quad (2)$$

3.3. TNF-α response studies in serum with 2D membrane assembly

Fig. 4(a) shows the DPV spectra obtained on Anti-TNF-α/FNAB/PC-Au electrode with single membrane for TNF-α concentrations (100 pg/ml–100 ng/ml) in undiluted serum. Serum was assumed to have negligible or no TNF-α and mention concentration was obtained by spiking serum with standard TNF-α solution. It is clear from the figure that sensor shows negligible response to serum, and some signal even at 100 pg/ml indicating specificity and high sensitivity. However, the curve for serum was not found to be flat line and slight rise in curve suggests the presence of TNF-α in very low concentration. Further, the increase in peak current with increasing spiked TNF-α concentration, revealed the successful binding of antigens and secondary tags. Increasing peak current with concentration may be attributed to the higher production of final electro-active product via conversion of 4-amino phenyl phosphate to 4-amino phenol by alkaline phosphatase. Zoom image of DPV curve for lower concentrations shown in Fig. 4(b) reveal clear signal till 100 pg/ml. Peak current for different concentration was normalized by subtracting the current value obtained for serum only and utilized for estimation of linear range, limit of detection and sensitivity of electrode. Calibration curve using normalized data from 3 sets shown in Fig. 4c suggest that the electrode can be used for sensing TNF-α linearly in 100 pg/ml – 100 ng/ml range, which could be characterized using the linear equation: ΔI (μA)=0.894 μA +0.194 μA/(ng/ml) $C_{\text{TNF-α}}$ (ng/ml). Results of Anti-TNF-α/FNAB/PC-Au electrode reveals the high sensitivity of 194 *nA*/(ng/ml), with r^2 of 0.994 and detection limit of 100 pg/ml. Error bars in figure for triplicate experiments reveals the consistency within 4% error for each concentration. Results suggest that Anti-TNF-α/FNAB/PC-Au electrode can be used successfully for testing TNF-α in undiluted serum and may be applied for developing highly sensitive biosensor for other proteins as well. Further, to improve the sensitivity and detection limit, two membranes in single assembly was utilized and tested (Fig. 5).

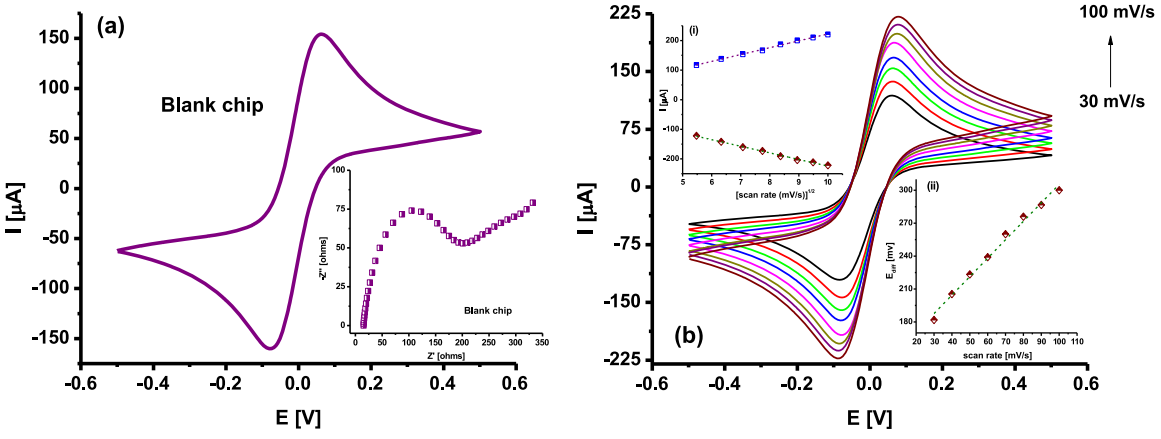

Fig. 3. Characterization of blank gold sensor chip (a) CV at scan rate of 50 mV/s and EIS measurements (inset) and (b) as a function of scan rates; inset (i) oxidation and reduction peak current response as a function of square root of scan rate, inset (ii) potential difference versus scan rate.

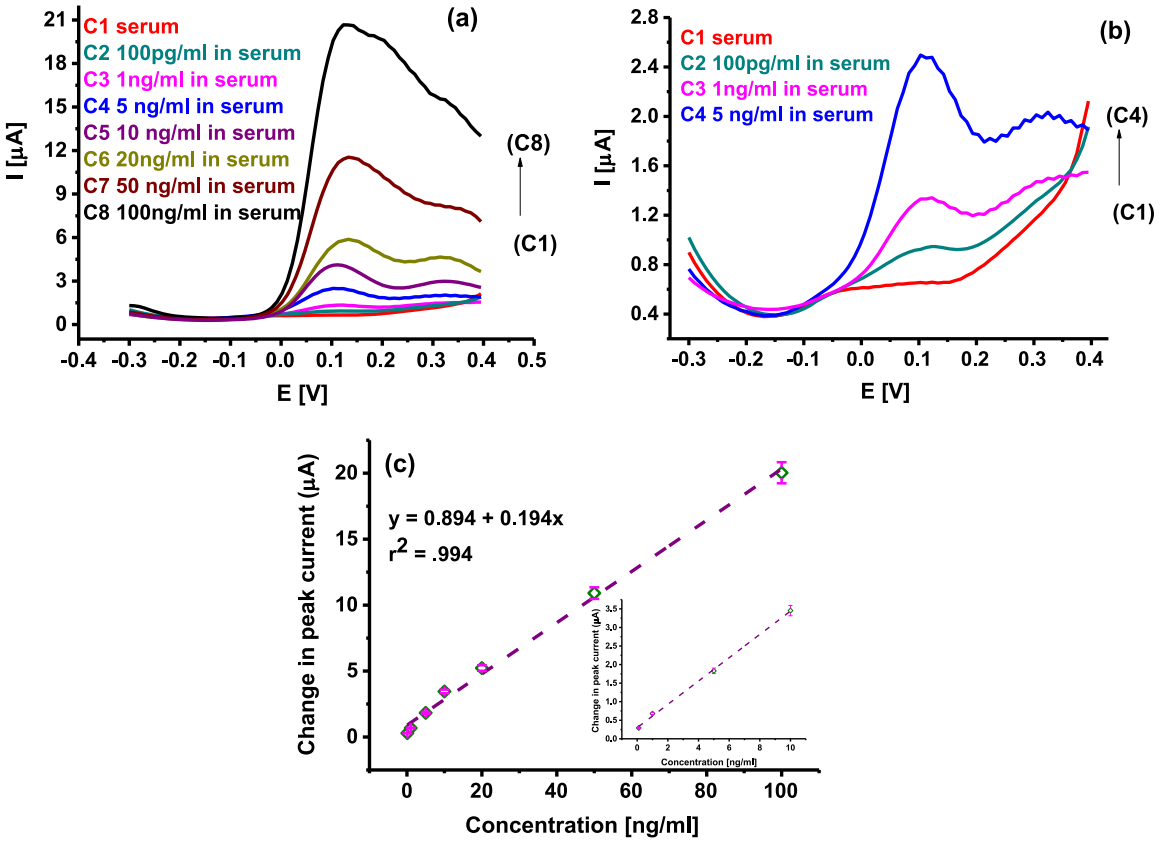

Fig. 4. (a) DPVs obtained on Anti-TNF-α/FNAB/PC-Au electrode with single membrane for TNF-α concentrations (100 pg/ml–100 ng/ml) in undiluted serum, (b) DPVs till 5 ng/ml concentration and (c) calibration curve obtained using normalized data, inset shows the enlarge image for lower concentrations.

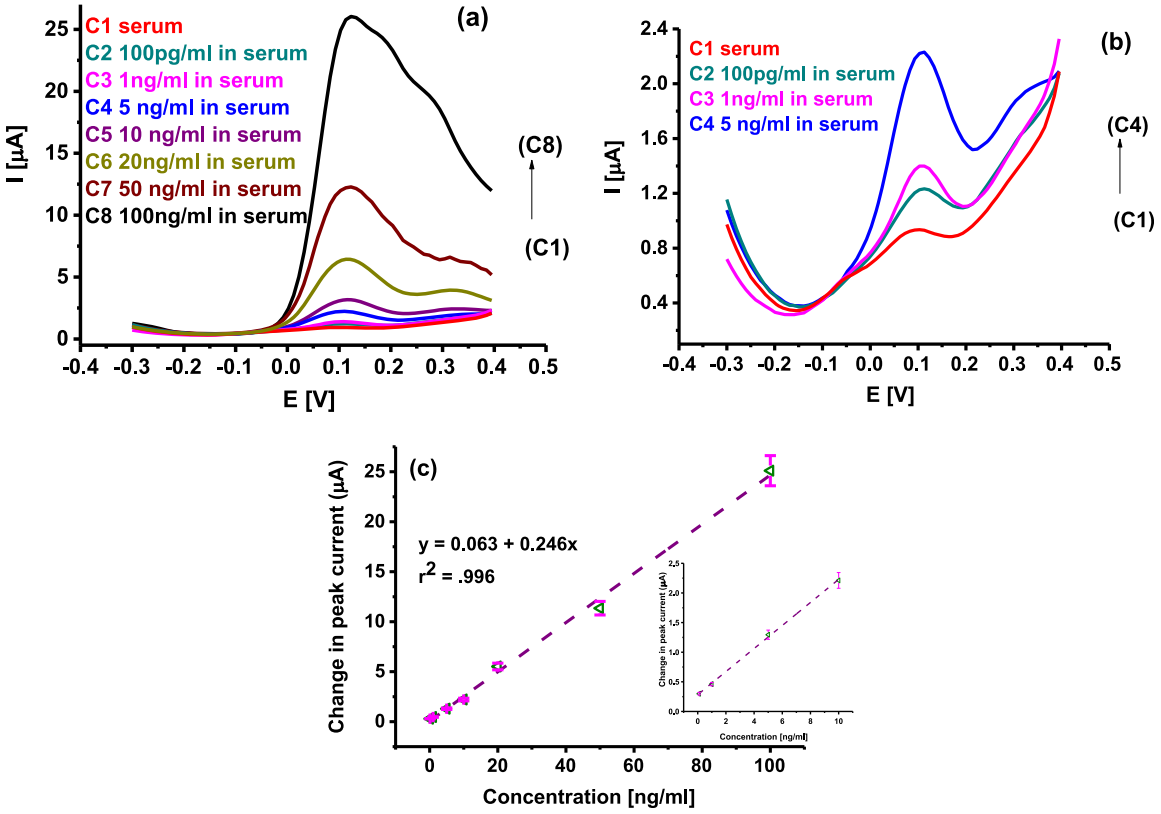

Fig. 5. (a) DPVs obtained on Anti-TNF-α/FNAB/PC-Au electrode with two membranes for TNF-α concentrations (100 pg/ml–100 ng/ml) in undiluted serum, (b) DPVs till 5 ng/ml concentration and (c) calibration curve obtained using normalized data, inset shows the enlarge image for lower concentrations.

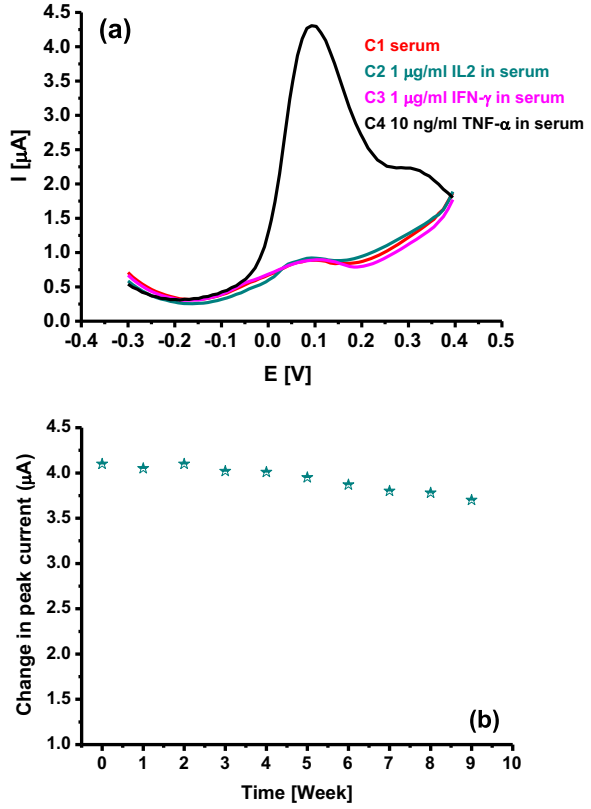

Fig. 6. (a) DPVs of a undiluted serum (C1), after 1 µg/ml of IL6 in serum incubation (C2), after 1 µg/ml of IFN-γ in serum incubation (C3), and after 10 ng/ml of TNF-α in serum incubation (C4), (b) Shelf life studies using 10 ng/ml of TNF-α over two month period.

Fig. 5(a) displays the DPV scans acquired on Anti-TNF-α/FNAB/PC-Au electrode with two membranes assembled in one system for detection of different TNF-α concentrations ranged 100 pg/ml–100 ng/ml spiked in undiluted serum. It is suggested from the figure that sensor showed slightly higher peak current as compared to when measured using single membrane based system. Zoom image in Fig. 5b for lower concentration suggest that use of the two membranes system enhances the response at 100 pg/ml, however some increase in background signal for serum only sample was also observed. This might be attributed to the overcrowding and physical entrapment of reagents between membranes. Also the observed rise DPV signal for serum only sample in single (Fig. 4b) and enhanced rise in double membrane (Fig. 5b) system may also be due to the presence of very low level of TNF-α in serum only sample. Although the doubled membrane system shows higher sensitivity, the singled membrane system offers a cleaner response, thus the rest of the studies were performed using single membrane based electrodes. For analyzing the data, normalization was performed by subtracting peak currents of the desired TNF- α concentration with that obtained from serum only. Calibration curve using normalized data from 3 sets were plotted (Fig. 5c) and the data suggested that the electrode can be used for TNF-α sensing linearly in 100 pg/ml–100 ng/ml concentrations range following the linear equation: ΔI (µA)=0.06 µA+0.24 µA/(ng/ml) $C_{\text{TNF-α}}$ (ng/ml). Further, results revealed the high sensitivity of 240 nA/(ng/ml), with r^2 of 0.996 and detection limit of 100 pg/ml. Triplicate sets of experiment suggested comparable response for all concentration and inside 6% error.

3.4. Interference from other cytokines and shelf life studies

It has been demonstrated that present sensor showed high selectivity toward TNF- α spiked in undiluted serum, however to confirm further selectivity and the effect of interference from other cytokines, measurements were made for serum spiked with other cytokines such as IL6 and IFN-γ at high concentration of 1 µg/ml and compared with response of 10 ng/ml TNF-α. Fig. 6a shows the DPV results of interference study from (i) undiluted serum, (ii) 1 µg/ml of IL6 in serum, (iii) 1 µg/ml of IFN-γ in serum, and (iv) 10 ng/ml of TNF-α in serum. It is clear from the figure that electrode does not show significant response to any other protein in serum or cytokines even at higher concentration and exhibit very good selective response in presence of TNF-α. Thus, Anti-TNF-α/FNAB/PC-Au electrode in off surface matrix with on-chip configuration offers a new platform for biosensor development to detect protein biomarkers in undiluted serum with high sensitivity. Further the DPV studies were performed to test the shelf life of the Anti-TNF-α/FNAB/PC-Au electrode over 2 month period at interval of one week. 10 ng/ml of TNF-α in serum was test every week on selected electrode from a set made at same time and kept in fridge till use. Fig. 6b shows the shelf life study graph in which the data suggest that Anti-TNF-α/FNAB/PC-Au electrode retain more than 90% of its initial value even after two months indicating good electrode stability. Electrodes prepared in the same set and prepared in different sets were also tested for 10 ng/ml of TNF-α in serum at same time and the results showed less than 5% variation, indicating controlled fabrication and sensor reproducibility.

4. Conclusion

In summary, 2D porous membrane as matrix in combination with on-chip testing present new electrochemical immunosensing platform for avoiding serum interference while achieving high specificity and improved detection sensitivity. Anti-TNF-α/FNAB/PC-Au electrode development described in this work by employing 2D porous membrane based off-surface matrix with on-chip measurement based system exhibited high sensitivity and selective measurement of TNF-α in undiluted serum in range of 100 pg/ml–100 ng/ml. The Anti-TNF-α/FNAB/PC-Au electrodes exhibited sensitivity of 194 nA/(ng/ml) for single membrane system with minimum detectable limit of 100 pg/ml. The Anti-TNF-α/FNAB/PC-Au electrode was found to be selective against other cytokines and serum proteins. Further, fabrication method was found reproducible and system was found to be selective over serum proteins, IL2 and IFN-γ and showed stability for over two-month period when stored at 4 °C in humid chamber. Similar to this other material membrane or PC membrane with lower or higher pore size can be studied for further improvement in response. Studies with 5 and 10 µm pore size are under study and results will be published in future. Moreover, prototype development for automation and multiplexing is in progress and will be evaluated in future.

Acknowledgment

Authors like to thank Science and Engineering Research Council of A*STAR (Agency for Science, Technology and Research), Singapore and JCO Grant (# 12302FG015) for supporting this work. Present addresses of S.K. Arya and M.K. Park are Biosensor Research Lab, Department of Electronic & Electrical Engineering, University of Bath, Claverton Down Road, Bath, North East Somerset BA2 7AY, Great Britain and One Biomed Pte. Ltd.,10 Anson road, #49-14, International plaza, Singapore 079903, respectively.

References

Arya, S.K., Bhansali, S., 2011. Chem. Rev. 111 (11), 6783–6809.
Arya, S.K., Kongsuphol, P., Wong, C.C., Polla, L.J., Park, M.K., 2014. Sens. Actuators B: Chem. 194, 127–133.
Arya, S.K., Park, M.K., 2014. Biosens. Bioelectron. 61, 260–265.
Arya, S.K., Park, M.K., Kongsuphol, P., Chung, J., 2016. In: WIPO, I.B.o. (Ed.). Agency for Science, Technology and Research, Singapore, WO2016/167724.
Arya, S.K., Pui, T.S., Wong, C.C., Kumar, S., Rahman, A.R.A., 2013. Langmuir 29 (22),

6770–6777.
Arya, S.K., Saha, S., Ramirez-Vick, J.E., Gupta, V., Bhansali, S., Singh, S.P., 2012. Anal. Chim. Acta 737, 1–21.
Arya, S.K., Solanki, P.R., Singh, R.P., Pandey, M.K., Datta, M., Malhotra, B.D., 2006. Talanta 69 (4), 918–926.
Arya, S.K., Solanki, P.R., Singh, S.P., Kaneto, K., Pandey, M.K., Datta, M., Malhotra, B.D., 2007. Biosens. Bioelectron. 22 (11), 2516–2524.
Bora, U., Sharma, P., Kumar, S., Kannan, K., Nahar, P., 2006. Talanta 70 (3), 624–629.
Bosnjakovic, A., Mishra, M.K., Han, H.J., Romero, R., Kannan, R.M., 2012. Anal. Chim. Acta 720, 118–125.
Chikkaveeraiah, B.V., Bhirde, A.A., Morgan, N.Y., Eden, H.S., Chen, X., 2012. ACS Nano 6 (8), 6546–6561.
Corrie, S.R., Coffey, J.W., Islam, J., Markey, K.A., Kendall, M.A.F., 2015. Analyst 140 (13), 4350–4364.
Fei, J., Dou, W., Zhao, G., 2015. RSC Adv. 5 (91), 74548–74556.
Felder, M., Kapur, A., Gonzalez-Bosquet, J., Horibata, S., Heintz, J., Albrecht, R., Fass, L., Kaur, J., Hu, K., Shojaei, H., Whelan, R.J., Patankar, M.S., 2014. Mol. Cancer 13 (1), 1–15.
Gan, N., Jia, L., Zheng, L., 2011a. J. Autom. Methods Manag. Chem. 2011, 7.
Gan, N., Jia, L., Zheng, L., 2011b. Int. J. Mol. Sci. 12 (11), 7410–7423.
Guo, Q., Li, X., Shen, C., Zhang, S., Qi, H., Li, T., Yang, M., 2015. Microchim. Acta 182 (7), 1483–1489.
Kaushik, A., Vasudev, A., Arya, S.K., Pasha, S.K., Bhansali, S., 2014. Biosens. Bioelectron. 53, 499–512.
Kokkinos, C., Economou, A., Prodromidis, M.I., 2016. TrAC Trends Anal. Chem. 79, 88–105.
Li, T., Si, Z., Hu, L., Qi, H., Yang, M., 2012. Sens. Actuators B: Chem. 171–172, 1060–1065.
Li, Y., Roy, W.V., Vereecken, P.M., Lagae, L., 2015. Nano/micro engineered and molecular systems (NEMS). In: Proceedings of the 2015 IEEE 10th International Conference. pp. 76–81.
Li, Z., Wang, Y., Wang, J., Tang, Z., Pounds, J.G., Lin, Y., 2010. Anal. Chem. 82 (16), 7008–7014.
Liu, Y., Liu, Y., Matharu, Z., Rahimian, A., Revzin, A., 2015a. Biosens. Bioelectron. 64, 43–50.
Liu, Y., Matharu, Z., Rahimian, A., Revzin, A., 2015b. Biosens. Bioelectron. 64, 43–50.
Mazloum-Ardakani, M., Hosseinzadeh, L., 2015. RSC Adv. 5 (87), 70781–70786.
Mazloum-Ardakani, M., Hosseinzadeh, L., Khoshroo, A., 2015. Electroanalysis 27 (11), 2518–2526.
Pan, L.-H., Kuo, S.-H., Lin, T.-Y., Lin, C.-W., Fang, P.-Y., Yang, H.-W., 2017. Biosens. Bioelectron. 89 (1), 598–605.
Pei, H., Wan, Y., Li, J., Hu, H., Su, Y., Huang, Q., Fan, C., 2011. Chem. Commun. 47 (22), 6254–6256.
Pui, T.S., Kongsuphol, P., Arya, S.K., Bansal, T., 2013. Sens. Actuators B: Chem. 181, 494–500.
Sadik, O.A., Aluoch, A.O., Zhou, A., 2009. Biosens. Bioelectron. 24 (9), 2749–2765.
Salimi, A., Khezrian, S., Hallaj, R., Vaziry, A., 2014. Anal. Biochem. 466, 89–97.
Sun, Z., Deng, L., Gan, H., Shen, R., Yang, M., Zhang, Y., 2013. Biosens. Bioelectron. 39 (1), 215–219.
Vasan, A.S.S., Mahadeo, D.M., Doraiswami, R., Huang, Y., Pecht, M., 2013. Front. Biosci., 39–71, (Scholar edition).
Vasudev, A., Kaushik, A., Bhansali, S., 2013. Biosens. Bioelectron. 39 (1), 300–305.
Wang, H., Wu, X., Dong, P., Wang, C., Wang, J., Liu, Y., Chen, J., 2014. Int. J. Electrochem. Sci. 9 (9), 12–21.
Wang, J., Liu, G., Engelhard, M.H., Lin, Y., 2006. Anal. Chem. 78 (19), 6974–6979.
Wei, Y., Li, Y., Li, N., Zhang, Y., Yan, T., Ma, H., Wei, Q., 2016. Biosens. Bioelectron. 79, 482–487.
Yin, Z., Liu, Y., Jiang, L.-P., Zhu, J.-J., 2011. Biosens. Bioelectron. 26 (5), 1890–1894.
Zhang, Y., Zhang, B., Ye, X., Yan, Y., Huang, L., Jiang, Z., Tan, S., Cai, X., 2016. Mater. Sci. Eng.: C 59, 577–584.